

Effective Spring Constant of Bubbles and Droplets

Phil Attard* and Stan J. Miklavcic†

Ian Wark Research Institute, University of South Australia, Mawson Lakes SA 5095, Australia

Received June 25, 2001. In Final Form: October 3, 2001

It is shown that gas bubbles and liquid droplets respond as hookean springs to applied loads in the experimental weak force regime. An analytic expression is obtained for the spring constant that is identical for both, linear in the surface tension γ , and logarithmically dependent on the lengths (the decay length of the interaction, the radius of the bubble or droplet, and the radius of the particle or probe). For acute interior contact angles greater than about 20° , it is typically in the range $0.8-1.2\gamma$, in agreement with published atomic force microscopy data, and it increases logarithmically for smaller contact angles. Analytic expressions are also obtained for the deformed profile, the extent of the dimple and of the interaction region, the wrapping radius, and the rupture force.

Introduction

The interaction of gas bubbles and liquid droplets with themselves or with particles or substrates is important in such diverse areas of manufacturing and technology as froth flotation, oil recovery, printing and deinking, and emulsion stability. Accordingly, in recent years, direct quantitative measurements of forces in well-defined model systems have been made. In particular, the atomic force microscope (AFM) has been used to measure the interaction of a colloid probe with an air bubble^{1–3} and with an oil droplet.^{4–8} Similarly, the deformation of fluid interfaces has been obtained theoretically under a variety of interactions.^{8–14} In the case of bubbles and droplets, the deformation is controlled by the surface tension and the pressure drop across the interface. In contrast, the deformation of elastic^{16,17} and viscoelastic^{18,19} solids is controlled by the bulk material properties of the particle.

This paper addresses the question of whether a bubble or droplet behaves as a simple hookean spring under a load applied by a particle or probe. If it does, then in an AFM measurement there will appear a region of constant

compliance with slope²⁰

$$\frac{\Delta x}{\Delta D} = \frac{k}{k_c + k} \quad (1)$$

where x is the cantilever deflection, D is the piezo drive distance, k is the spring constant of the fluid interface, and k_c is the cantilever spring constant. There is strong experimental evidence for the existence of such a regime, and following Ducker et al.,¹ a number of authors have interpreted their data in terms of such a simple spring.^{3,4,7} Particularly convincing is the extensive study of Hartley et al. for oil droplets, which gave a value for the effective spring constant that is close to the surface tension of the oil–water interface.⁷ Closely related to bubbles and droplets are fluid membranes, and Evans and co-workers developed an ultrasensitive force measuring device based upon the notion that the effective spring of a vesicle or cell membrane existed and was linearly proportional to the surface tension.¹⁵

In contrast to the experimental evidence, the recent theoretical papers that have addressed this very question have reached differing conclusions. Aston and Berg⁸ conclude that “a fluid interface ... is not accurately treated as a hookean spring”. A similar conclusion was made by Bhatt et al.,¹⁴ who state that “the assumption of linear elasticity for fluid bubbles or drops is not valid”. On the other hand, on the basis of their numerical calculations, Chan et al.¹³ conclude that “a hookean force law is valid for low to moderate distortions”, although they were unable to quantify the value of the spring constant or the regime in which the simple spring model was accurate.

This paper analyzes the problem in detail using a perturbation treatment about the spherical profile of the undeformed interface. We conclude that bubbles and droplets behave as simple springs, in accord with Hooke’s law. We establish that the result is applicable for weak forces such as those that are used in the experimental measurements and those that apply in practical situations.

(20) Strictly speaking, the definition of a hookean or linear spring is that the extension of the spring, in this case the position of the interface Δz , is linear in the force, in this case $\Delta F = k_c \Delta x$. Equation 1 holds when $\Delta z = \Delta D$, which is the case when the change in separation is negligible compared to the change in drive distance. In the initial weak force regime, the former is comparable to the latter and eq 1 is violated. In other words, eq 1 is a sufficient but not necessary condition for the bubble or droplet to behave as a hookean spring.

* To whom correspondence should be addressed at phil.attard@unisa.edu.au.

† Permanent address: Department of Science and Technology, Campus Norrköping, Linköping University, Bredgatan 33-34, S-601 74 Norrköping, Sweden.

- (1) Ducker, W. A.; Xu, Z.; Israelachvili, J. N. *Langmuir* **1994**, *10*, 3279.
- (2) Butt, H.-J. *J. Colloid Interface Sci.* **1994**, *166*, 109.
- (3) Preuss, M.; Butt, H.-J. *Langmuir* **1998**, *14*, 3164.
- (4) Basu, S.; Sharma, M. M. *J. Colloid Interface Sci.* **1996**, *181*, 443.
- (5) Mulvaney, P.; Perera, J. M.; Biggs, S.; Grieser, F.; Stevens, G. W. *J. Colloid Interface Sci.* **1996**, *183*, 614.
- (6) Snyder, B. A.; Aston, D. E.; Berg, J. C. *Langmuir* **1997**, *13*, 590.
- (7) Hartley, P. G.; Grieser, F.; Mulvaney, P.; Stevens, G. W. *Langmuir* **1999**, *15*, 7282.
- (8) Aston, D. E.; Berg, J. C. *J. Colloid Interface Sci.* **2001**, *235*, 162.
- (9) Miklavcic, S. J.; Horn, R. G.; Bachmann, D. J. *J. Phys. Chem.* **1995**, *99*, 16357.
- (10) Bachmann, D. J.; Miklavcic, S. J. *Langmuir* **1996**, *12*, 4197.
- (11) Miklavcic, S. J. *Phys. Rev. E* **1996**, *54*, 6551.
- (12) Miklavcic, S. J. *Phys. Rev. E* **1998**, *57*, 561.
- (13) Chan, D. Y. C.; Dagastine, R. R.; White, L. R. *J. Colloid Interface Sci.* **2001**, *236*, 141.
- (14) Bhatt, D.; Newman, J.; Radke, C. J. *Langmuir* **2001**, *17*, 116.
- (15) Evans, E.; Ritchie, K.; Merkel, R. *Biophys. J.* **1995**, *68*, 2580.
- (16) Attard, P.; Parker, J. L. *Phys. Rev. A* **1992**, *46*, 7959.
- (17) Attard, P. *J. Phys. Chem. B* **2000**, *104*, 10635.
- (18) Attard, P. *Phys. Rev. E* **2001**, *63*, 061604.
- (19) Attard, P. *Langmuir* **2001**, *17*, 4322.

We obtain an expression for the effective spring constant and show that it is linear in the surface tension, with a proportionality constant slightly less than unity for typical values of the system parameters. We also show that the result holds in general and is independent of the specific force law.

General Formalism

The constrained thermodynamic potential²¹ for a bubble or droplet interacting with a particle is^{22,23}

$$\mathcal{G}[z(r)] = H + p_0 V + \gamma A - \Delta\gamma A_s + \Omega \quad (2)$$

The potential is of course constrained with respect to the nonequilibrium profile $z(r)$. The equilibrium profile, $\bar{z}(r)$, is the one that minimizes the constrained thermodynamic potential, and the minimum value is called the Gibbs potential, $\bar{\mathcal{G}}(N, p_0, T, \gamma, \Delta\gamma) = \mathcal{G}[\bar{z}(r)]$.²¹ Here $H(N, V, T)$ is the bulk Helmholtz free energy of the bubble or drop, p_0 is the external atmospheric pressure, γ is the surface tension of the fluid interface, $\Delta\gamma = \gamma \cos \theta$ is the difference in surface energies of the solid substrates, θ being the interior contact angle, and gravity is neglected. The drop or bubble has the volume

$$V = \int_0^s dr 2\pi r z(r) \quad (3)$$

the fluid interfacial area

$$A = \int_0^s dr 2\pi r W(r) \quad (4)$$

and the contact area $A_s = \pi s^2$. Here r is the radial distance from the axis of cylindrical symmetry of the drop or bubble, $z(r)$ is the local height of the drop or bubble above the substrate, $W(r) = [1 + z'(r)^2]^{1/2}$ is the element of area, and s is the contact radius, $z(s) = 0$. These expressions assume that for each r there is a unique $z(r)$, which is true for acute contact angles.

The above expression is essentially equivalent to that used by earlier workers,^{8–14} with three differences. First, the constrained thermodynamic potential approach used here avoids Lagrange multipliers and instead invokes physical quantities fixed by a reservoir;²¹ the constrained thermodynamic potential has the physical interpretation of the constrained total entropy of the whole system. Second, the Helmholtz free energy is invoked here to reflect the correct physical condition for thermodynamic stability, namely that the number of molecules in the bubble or droplet is fixed on the time scale of the experiment.^{22,23} (The alternative assumption that it is the volume that is fixed is not true for gas bubbles, although it is a common approximation for liquid droplets.) The present formalism enables gas bubbles and liquid droplets to be treated equivalently, simultaneously, and exactly.

Third, the particle enters in the above through its interaction free energy with the drop or bubble,²⁴

$$\Omega = \int_0^s dr 2\pi r W(r) \omega(h(r)) \quad (5)$$

where $\omega(h)$ is the interaction free energy per unit area between planar surfaces separated by h and $h(r)$ is the

closest distance from the fluid interface at $z(r)$ to the particle surface,

$$h(r) = -R_p + \sqrt{r^2 + (R_p + y - z(r))^2} \quad (6)$$

where R_p is the radius of the particle and y is the position of the surface of the particle on the axis. This approximation is almost identical to the Derjaguin approximation used by earlier workers^{8–14} except that the latter neglects the area factor $W(r)$ and it also approximates $h(r)$ by the vertical distance between the fluid interface and the particle surface at r . The present expression is arguably more consistent at large separations and also in the wrapping regime where the surfaces are nearly parallel. When the fluid interface is convex and the separation is small compared to the range of the interaction (weak but not too weak forces), the present expression and the Derjaguin approximation are identical. The influence of this more rigorous expression for the interaction term is explored in greater detail by us in ref 24.

In general, the force on the particle is the negative derivative of the interaction free energy with respect to the particle's position y . It also equals the derivative with respect to the position of the substrate or with respect to a uniform displacement of the interface, which may be denoted by z . That is, the force may be written equivalently as

$$\begin{aligned} F &= \frac{-\partial\Omega}{\partial y} = \frac{\partial\Omega}{\partial z} \\ &= \int_0^s dr 2\pi r W(r) \frac{\partial\omega(h(r))}{\partial z(r)} \end{aligned} \quad (7)$$

The last equality follows because $z(r)$ occurs in the combination $y - z(r)$ in the definition of $h(r)$. The dependence of the equilibrium profile on the position of the probe may be ignored in the differentiation because of the variational nature of the constrained thermodynamic potential.^{22,23}

The equilibrium profile satisfies the Euler–Lagrange equations, $\delta\mathcal{G}/\delta z(r)|_{\bar{z}(r)} = 0$ or

$$\frac{\partial f(r)}{\partial z(r)} - \frac{d}{dr} \frac{\partial f(r)}{\partial z'(r)} = 0 \quad (8)$$

where $f(r) \equiv f(r, z(r), z'(r))$ is the free energy density. Here and henceforth the overline on the profile is dropped; whenever the Euler–Lagrange equation is invoked, it will be taken as understood that it is the equilibrium profile that appears. Explicitly, this is

$$\begin{aligned} \frac{d}{dr} \left\{ \frac{2\pi r z'(r)}{\sqrt{1 + z'(r)^2}} [\gamma + \omega(h(r))] \right\} = \\ -2\pi r \Delta p + 2\pi r W(r) \frac{\partial\omega(h(r))}{\partial z(r)} \end{aligned} \quad (9)$$

where $\Delta p = p_{in} - p_0$ is the pressure drop. One sees that the interaction free energy augments the surface tension and, for a repulsive interaction, effectively stiffens the interface in the contact region. This effect is neglected in the Derjaguin approach.

Regimes

We shall consider particles of radius R_p and bubbles or droplets of radius R_0 , with the latter much larger than the former, $R_p \ll R_0$. We shall give results for acute interior

(21) Attard, P. *J. Stat. Phys.* **2000**, *100*, 445.

(22) Attard, P. *Langmuir* **1996**, *12*, 1693.

(23) Attard, P. *Langmuir* **2000**, *16*, 4455.

(24) Miklavcic, S. J.; Attard, P. *J. Phys. A* **2001**, *34*, 7849.

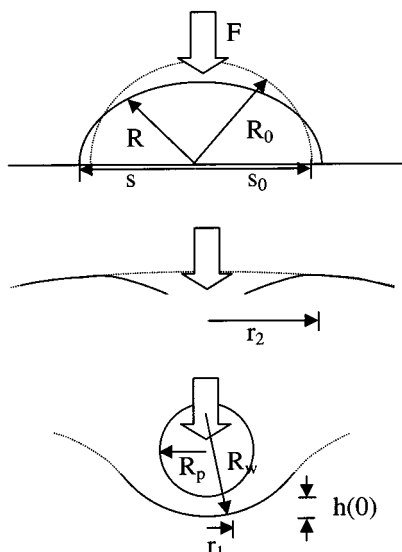


Figure 1. Deformation of a droplet or bubble by an applied load. The three regimes are shown at successively higher magnifications.

contact angles; the analysis is more tedious for obtuse contact angles (because the mapping from r to z is no longer one to one), with similar results being expected. We shall consider repulsive interactions (positive applied load), so that $z(r) < z_0(r)$, $r \approx 0$, where $z_0(r)$ is the undeformed profile. This last restriction is not important, and the results below apply as well to attractive interactions if F is replaced by $|F|$ where necessary.

To calculate the total deformation due to an applied load, we define two boundaries that separate the problem into three regimes (see Figure 1). The inner boundary r_1 represents the maximum extent of the region that directly interacts with the particle or probe (i.e. $\omega(h(r)) = 0$, $r \geq r_1$). For an exponentially decaying interaction pressure with decay length κ^{-1} , we shall show that $r_1 \sim \sqrt{2R_p/\kappa}$, eq 50 below. The outer boundary r_2 is the rim of the dimple formed by the applied load; it is the radius of the circle of peaks of the deformed interface. We shall show that $r_2 \sim \sqrt{FR_0/2\pi\gamma}$, eq 12 below.

Our analysis is valid in the weak force regime,

$$F \ll 2\pi\gamma R_p \quad (10)$$

This is not a very great restriction because the bubble or drop will rupture unless $F < 2\pi\gamma R_p$ (see ref 24 and eq 38 below). Typical experimental data have $F_{\max}/2\pi\gamma R_p = 10^{-3}$ to 10^{-2} .^{3,7,8}

Location of Rim

A first integral of the Euler–Lagrange equation (eq 9) from 0 to $r > r_1$ yields

$$\frac{2\pi\gamma r z'(r)}{\sqrt{1 + z'(r)^2}} = F - \pi r^2 \Delta p, \quad r > r_1 \quad (11)$$

where eq 7 has been used, as well as the fact that $\omega(h(r)) = 0$ for $r \geq r_1$. This is an exact result which shows that beyond the particle the profile of the deformed interface is determined by the load in total and does not depend on the detailed surface interactions or force law.

Now the position of the maximum in the profile is defined by $z'(r_2) = 0$. Evidently, the right-hand side vanishes here,

which yields

$$r_2 = \sqrt{\frac{F}{\pi\Delta p}} = \sqrt{\frac{FR}{2\pi\gamma}} \quad (12)$$

The second equality defines the deformed curvature R (see next). To leading order in F , this is $r_2 \sim [FR_0/2\pi\gamma]^{1/2}$.

Although we restrict our attention to acute interior contact angles in this paper, it's worth mentioning that for the case of obtuse angles the maximum lateral extent t of the bubble or drop can be derived by similar analysis. Since $z(t) = -\infty$, the exact Euler–Lagrange equation yields

$$t = \frac{R}{2} [1 + \sqrt{1 + 2F/\pi\gamma R}] \\ \sim R + F/2\pi\gamma + \mathcal{O}F^2 \quad (13)$$

Outer Regime

In the region beyond the dimple, $r \gtrsim r_2$, the pressure term on the right-hand side of eq 11 dominates, and the force acts as a perturbation on the profile. Accordingly, we may expand everything to linear order in F here. Using a subscript zero to denote the undeformed interface, the radius of the initially hemispherical droplet or bubble is R_0 , and the initial pressure drop is $\Delta p_0 = 2\gamma/R_0$. We define the mean radius of curvature of the deformed interface far from the dimple by $R = 2\gamma/\Delta p$ and seek the first-order correction to the undeformed radius

$$\rho = R - R_0 \quad (14)$$

The perturbation ρ , which is linearly proportional to the force, will be shown to be positive. Since

$$\Delta p = \Delta p_0 + \frac{\partial p_{\text{in}}}{\partial V} \Delta V \\ = \frac{2\gamma}{R_0} - \frac{1}{V_0 \chi_T} \Delta V \quad (15)$$

one has

$$\rho = \frac{R_0^2}{2\gamma V_0 \chi_T} \Delta V \quad (16)$$

Here χ_T is the isothermal compressibility of the gas comprising the bubble or of the liquid comprising the droplet. An explicit expression for ΔV will be obtained shortly.

An expansion of the exact integrated Euler–Lagrange equation (eq 11) to linear order in F and ρ yields

$$z'(r) = \frac{(F/2\pi\gamma r) - (r/R)}{\sqrt{1 - [(F/2\pi\gamma r) - (r/R)]^2}} \\ \sim \frac{-r/R_0}{\sqrt{1 - r^2/R_0^2}} + \frac{\rho r/R_0^2}{[1 - r^2/R_0^2]^{3/2}} + \\ \frac{F/2\pi\gamma r}{[1 - r^2/R_0^2]^{3/2}} + \mathcal{O}F^2 \\ \equiv z'_0(r) + \epsilon'(r) \quad (17)$$

The function $\epsilon'(r)$ is linear in F and ρ , and hence so is $\epsilon(r)$, which facts are used several times below. This expansion is valid for $r \gtrsim r_2$.

The profile of the undeformed hemisphere is

$$z_0(r) = z_0(0) - R_0 + \sqrt{R_0^2 - r^2} \quad (18)$$

with the contact radius on the substrate being given by

$$s_0^2 = 2R_0z_0(0) - z_0(0)^2 \quad (19)$$

and the interior contact angle obeying

$$\sin \theta = \frac{s_0}{R_0} \quad (20)$$

All properties of the undeformed hemispherical bubble or droplet may be written in terms of R_0 and θ .

The deformed profile itself is obtained by integration, and to linear order one has

$$\begin{aligned} z(r) &= \int_s^r dr z'(r) \\ &\sim \int_{s_0}^r dr [z'_0(r) + \epsilon'(r)] + [s_0 - s]z'_0(s_0) + \mathcal{O}F^2 \end{aligned} \quad (21)$$

using Leibnitz's rule, and also the facts that $z(s) = 0$ and that $s - s_0 \sim \mathcal{O}F$. The integral of the undeformed profile is the $z_0(r)$ given above.

Since the contact angle is unchanged by the applied load, and since it may be written as a function of the gradient of the profile at contact, $\tan \theta = -z'(s)$, we have

$$\begin{aligned} z'_0(s_0) &= z'(s) \\ &\sim z'_0(s) + \epsilon'(s) + \mathcal{O}F^2 \\ &= z'_0(s_0) + [s - s_0]z''_0(s_0) + \epsilon'(s) \end{aligned} \quad (22)$$

That is, the change in contact radius due to the applied force is

$$s - s_0 \sim -\epsilon'(s)/z''_0(s_0) + \mathcal{O}F^2 \quad (23)$$

It is straightforward to show that

$$z''_0(s_0) = -1/R_0 \cos^3 \theta \quad (24)$$

and that

$$\epsilon'(s) = \frac{\rho \sin \theta}{R_0 \cos^3 \theta} + \frac{F/2\pi\gamma R_0}{\sin \theta \cos^3 \theta} + \mathcal{O}F^2 \quad (25)$$

since $\epsilon'(s) - \epsilon'(s_0) = \mathcal{O}F^2$.

The integration for the profile perturbation, eq 17, may be performed analytically (see eqs 2.266 and 2.268 of ref 25),

$$\begin{aligned} \epsilon(r) - \epsilon(s_0) &= \left[\frac{F}{2\pi\gamma} + \rho \right] \left[\frac{1}{\sqrt{1 - r^2/R_0^2}} - \frac{1}{\sqrt{1 - s_0^2/R_0^2}} \right] + \\ &\quad \frac{F}{2\pi\gamma} \ln \left[\frac{r(1 + \sqrt{1 - s_0^2/R_0^2})}{s_0(1 + \sqrt{1 - r^2/R_0^2})} \right] \end{aligned} \quad (26)$$

Hence, to leading order in F the deformed profile is given

(25) Gradshteyn, I. S.; Ryzhik, I. M. *Tables of Integrals, Series, and Products*; Academic: San Diego, CA, 1980.

by

$$z(r) = z_0(r) + R_0\epsilon'(s) \sin \theta \cos^2 \theta + \epsilon(r) - \epsilon(s_0) \quad (27)$$

With these results we can now evaluate the change in volume of the drop or bubble to linear order in the force, and hence the change in radius ρ . The change in volume is

$$\begin{aligned} \Delta V &= \int_0^s dr 2\pi r z(r) - \int_0^{s_0} dr 2\pi r z_0(r) \\ &\sim [s - s_0]2\pi s_0 z_0(s_0) + \mathcal{O}F^2 + \int_0^{r_0} dr 2\pi r \Delta z(r) + \\ &\quad \int_{r_2}^{s_0} dr 2\pi r \Delta z(r) \\ &\sim \int_0^{s_0} dr 2\pi r [\epsilon(r) - \epsilon(s_0) + \\ &\quad R_0\epsilon'(s_0) \sin \theta \cos^2 \theta] + \mathcal{O}F^2 \\ &= \pi s_0^2 R_0 \epsilon'(s_0) \sin \theta \cos^2 \theta - \int_0^{s_0} dr \pi r^2 \epsilon'(r) \end{aligned} \quad (28)$$

Here we have written $\Delta z(r) = z(r) - z_0(r)$. On the right-hand side of the second equality, the first term is zero (since the profile is zero at contact), and the second term may be neglected because it is $\mathcal{O}F^2$ (since r_2 scales with the square root of the force). The first term on the right-hand side of the final equality may be written

$$\pi s_0^2 R_0 \epsilon'(s_0) \sin \theta \cos^2 \theta = \pi R_0^2 (a\rho + bF/2\pi\gamma) \quad (29)$$

where $a \equiv \sin^4 \theta / \cos \theta$ and $b \equiv \sin^2 \theta / \cos \theta$. The final term in the last line of the equation for ΔV follows upon integration by parts. After integration and some manipulation, it may be written

$$- \int_0^{s_0} dr \pi r^2 \epsilon'(r) = \pi R_0^2 (cF/2\pi\gamma + d\rho) \quad (30)$$

where $c \equiv (\cos \theta - 1) / \cos \theta$ and $d \equiv [2 \cos \theta - 2 - \sin^2 \theta / \cos \theta]$. Accordingly, one may write the change in volume as $\Delta V = \pi R_0^2 [(a + d)\rho + (b + c)F/2\pi\gamma]$, and hence the change in radius of the drop or bubble is given by

$$\begin{aligned} \rho &= \frac{\pi R_0^4}{2\gamma V_0 \chi_T} \left[(b + c) \frac{F}{2\pi\gamma} + (a + d)\rho \right] \\ &= \frac{\pi R_0^4}{2\gamma V_0 \chi_T} (b + c) \frac{F}{2\pi\gamma} \\ &\quad \frac{1}{1 - \frac{\pi R_0^4}{2\gamma V_0 \chi_T} (a + d)} \end{aligned} \quad (31)$$

We now show that the change in mean curvature is identical for liquid drops and gas bubbles. For a bubble we use the ideal gas equation of state, in which case the compressibility is $\chi_T^{-1} = p_{\text{in}} \approx p_{\text{atm}}$. The approximate equality of these two holds in common cases. For example, millimeter-sized bubbles in water have $2\gamma/R_0 p_{\text{atm}} = 144 \times 10^{-5} \ll 1$. With the volume of the bubble being $V_0 = (\pi/3)R_0^3(1 - \cos \theta)^2(2 + \cos \theta)$, the dimensionless parameter that appears in the denominator and numerator of the expression for ρ is

$$\frac{\pi R_0^4}{2\gamma V_0 \chi_T} \approx \frac{3p_{\text{atm}} R_0^2 / 2\gamma}{(1 - \cos \theta)^2 (2 + \cos \theta)} \gg 1 \quad (32)$$

Hence, for gas bubbles we may as well take $\chi_T = 0$, which

is exactly the definition of an incompressible liquid. We conclude that gas bubbles and liquid droplets behave identically and that the change in the mean radius of curvature is in both cases

$$\begin{aligned}\rho &\approx -\frac{b+c}{a+d} \frac{F}{2\pi} \\ &= \frac{1-\cos\theta}{2-\cos\theta-\cos^3\theta} \frac{F}{2\pi\gamma}\end{aligned}\quad (33)$$

We now have an expression for the change in the radius of curvature, which in conjunction with eqs 25 and 26 gives explicitly the deformed profile, eqs 27, in the region $r_2 \lesssim r < R$. In the region of the dimple rim, since $r^2/R_0^2 = \mathcal{O}(F)$, this result to leading order in F is

$$z(r) = z_0(r) + \frac{F}{2\pi\gamma} \frac{3-3\cos\theta+\cos^2\theta-\cos^3\theta}{2-\cos\theta-\cos^3\theta} + \frac{F}{2\pi\gamma} \ln\left[\frac{r}{2R_0} \frac{1+\cos\theta}{\sin\theta}\right] + \mathcal{O}(F^2)\quad (34)$$

Dimple Regime

The gradient of the profile is small near r_2 , $|z'(r)| \ll 1$. In fact, for weak forces this holds everywhere within the dimple rim as well. Hence, an expansion to linear order in $z'(r)$ of the exact integrated Euler–Lagrange equation (eq 11) yields

$$z'(r) = \frac{F}{2\pi\gamma R} - \frac{r}{R}, \quad r_1 < r \lesssim r_2\quad (35)$$

Hence, within and beyond the dimple the deformed profile is given by

$$\begin{aligned}z(r) &= \frac{F}{2\pi\gamma} \ln r - \frac{r^2}{2R} + \text{constant} \\ &= \frac{F}{2\pi\gamma} \ln r - \frac{r^2}{2R_0} + \text{constant}, \quad r_1 < r \lesssim r_2\end{aligned}\quad (36)$$

where a term of $\mathcal{O}(F^2)$ has been neglected in the final line. Comparing this with the solution in the outer region $r_2 \lesssim r \ll R_0$, eq 34, one sees that they have an overlapping regime of validity (since $z_0(r) = z_0(0) - r^2/2R_0$, $r \ll R_0$). The reason is that the profile remains flat beyond the dimple rim, which is the region in which eq 34 is valid. Hence, one concludes that eq 34 is valid not only beyond but also within the dimple, $r_1 < r \ll R_0$.

Condition for Rupture

For small radii, $r \approx r_1$, the pressure drop term is negligible, and in this case the gradient of the profile is given by

$$z'(r) = \frac{F/2\pi\gamma}{\sqrt{1-(F/2\pi\gamma)^2}}, \quad r \gtrsim r_1\quad (37)$$

This places a limit on the maximum force that can be applied without rupturing the bubble or drop,

$$F < 2\pi\gamma_1 \lesssim 2\pi R_p \gamma\quad (38)$$

This is a sufficient condition for rupture; an instability in the profile could occur at smaller forces than given by this.²⁴

Wrapping Regime

The first integral of the exact Euler–Lagrange equation (eq 9) in the region where the interaction between the interface and the particle is non-negligible may be written

$$\begin{aligned}\pi r^2 \Delta p + \frac{2\pi r z'(r)}{\sqrt{1+z'(r)^2}} [\gamma + \omega(h(r))] &= \\ \int_0^r dr 2\pi r \sqrt{1+z'(r)^2} \frac{\partial \omega(h(r))}{\partial z(r)}\end{aligned}\quad (39)$$

It is obvious that the profile is a quadratic function of r near the origin, and the coefficient may be written in terms of the wrap radius R_w ,

$$z(r) \sim z(0) + \frac{r^2}{2R_w} + \mathcal{O}(r^4), \quad r \rightarrow 0\quad (40)$$

The radius of curvature in the wrapping regime is measured externally to the bubble or droplet, which is the opposite convention to that used for the radius of the bubble or droplet itself. For small loads, $R_w \rightarrow -R_0$, and for large loads, $R_w \rightarrow R_p$. Expanding eq 39 to leading order, one obtains

$$\begin{aligned}\frac{2\pi\gamma r^2}{R} + \frac{2\pi r^2}{R_w} [\gamma + \omega_0] + \mathcal{O}(r^4) &\sim \\ \int_0^r dr 2\pi r [1 + \mathcal{O}(r^2)] [p_0 + \mathcal{O}(r^2)] &\sim \\ \pi r^2 p_0 + \mathcal{O}(r^4)\end{aligned}\quad (41)$$

where $p_0 \equiv p(h(0)) = -\omega'(h(0))$ and $\omega_0 \equiv \omega(h(0))$ and $h_0 \equiv h(0)$. Here we have used the fact that $\partial h(r)/\partial z(r) \sim 1 + \mathcal{O}(h_0/R_p)$, with $h_0 \ll R_p$. Hence,

$$R_w^{-1} = \frac{-1}{R} \frac{\gamma}{\gamma + \omega_0} + \frac{p_0}{2[\gamma + \omega_0]}\quad (42)$$

This is exactly what one would expect, since p_0 represents the change in pressure at the apex due to the interactions with the particle or probe, and $\gamma + \omega_0$ represents the effective surface tension of the bubble or drop in the interaction region.

Now one must have that $R_w \geq R_p + h(0) \approx R_p$. Since for an electric double layer force of decay length κ^{-1} , $p_0 = \kappa\omega_0$, and $\kappa R_p \ll 1$, one concludes that h_0 must be such that $\omega_0 \ll \gamma$. (The proof is based upon an argument *ad absurdum*: if $\gamma \lesssim \omega_0$, then the denominator in eq 42 would be $\mathcal{O}(\kappa^{-1})$ times the numerator, and the right-hand side would be very much less than the left-hand side.) In other words, the stiffening of the interface by the interaction is practically negligible. Hence, the wrap radius as a function of separation is given by $R_w^{-1} = -R^{-1} + p(h(0))/2\gamma$. The smallest that the dimple radius can be is equal to the particle radius, and hence the maximum pressure that can be exerted is

$$p_{\max} = 2\gamma R_p\quad (43)$$

where R_0^{-1} has been neglected in comparison to the reciprocal of the particle radius. This also defines the minimum separation.

In view of the quadratic nature of $z(r)$ near the apex, the local separation is

$$h(r) = h_0 + r^2[R_p^{-1} - R_w^{-1}]/2 + \mathcal{O}(r^4/R_p^3) \quad (44)$$

Since the boundary of the inner region is defined such that $\omega(r_1) = 0$, the force is given by

$$F = \int_0^{r_1} dr 2\pi r \sqrt{1 + (r/R_w)^2} p(h(r)) \\ \sim \frac{2\pi}{\kappa[R_p^{-1} - R_w^{-1}]} p_0 + \mathcal{O}(r_1/R_w)^2 \quad (45)$$

This relates the peak pressure to the applied load and the wrapping radius. Accordingly, eq 42 with ω_0 neglected may be written

$$R_w^{-1} = p_0/2\gamma - R^{-1} \\ = \frac{F\kappa}{4\pi\gamma}[R_p^{-1} - R_w^{-1}] - R_0^{-1} + \rho/R_0^2 \quad (46)$$

The term ρ/R_0^2 is in practice of the order of $\kappa^{-1}R_p/R_0^2 \approx 10^{-7}$, times smaller than the first term on the right-hand side, and hence it may be neglected. Solving this gives for the wrap radius

$$R_w = -R_0 \frac{1 + f\kappa R_p/2}{1 - f\kappa R_0/2} \quad (47)$$

where $f \equiv F/2\pi\gamma R_p$. In practice $0 \lesssim f \lesssim 10^{-2}$, $\kappa R_p \approx 10^3$, and $\kappa R_0 \approx 10^5$. Hence, one sees that the wrap radius varies between $-R_0$ and R_p , as one would expect. To leading order in the force, the wrapping curvature is

$$R_w^{-1} \sim -R_0^{-1} + F\kappa/4\pi\gamma R_p + \mathcal{O}(F^2) \quad (48)$$

where terms of order R_p/R_0 have been neglected.

The boundary of the wrapping regime may be determined by matching the slopes of the inner and outer profiles. That is

$$\frac{r_1}{R_w} = \frac{F}{2\pi\gamma r_1} - \frac{r_1}{R_0} \quad (49)$$

with solution

$$r_1^2 = 2R_p\kappa^{-1} \frac{1 + F\kappa/4\pi\gamma}{1 + R_p/R_0} \sim 2R_p\kappa^{-1} + \mathcal{O}(F) + \mathcal{O}(R_p/R_0) \quad (50)$$

This shows that when $\kappa R_p \gg 1$, the particle interacts directly with the interface over a much smaller region than its cross section.

This is the only stage that the interaction law enters the analysis. If the interaction law is unknown, or if the repulsion is not due to an electric double layer (e.g., contact in air), then one can take $r_1 \approx R_p$ to obtain a reasonably good estimate of the deformation and spring constant of the interface.

The total deformation of the bubble or drop on the central axis in eq 40 is determined from the continuity of the

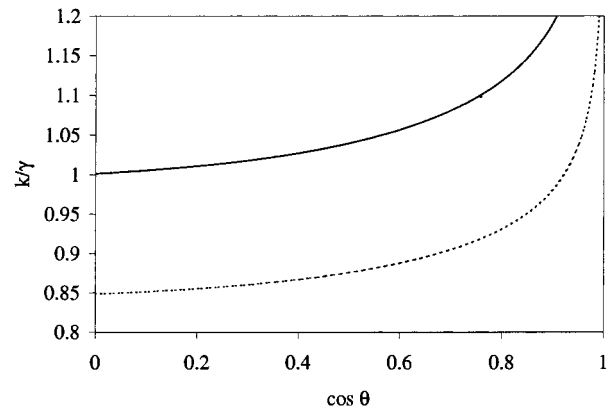


Figure 2. Spring constant of a fluid interface as a function of the interior contact angle. The ratio of length scales is $R_p\kappa^{-1}/R_0^2 = 10^{-6}$ (full curve) and 10^{-7} (dotted curve).

profile at r_1 . Using eq 34 for $z(r_1^+)$, one has

$$z(0) = z(r_1^+) - \frac{r_1^2}{2R_w} \\ = z_0(0) + \frac{F}{4\pi\gamma} \left\{ \ln \left[\frac{R_p}{2\kappa R_0^2} \frac{(1 + \cos \theta)^2}{\sin^2 \theta} \right] + \frac{4 - 5 \cos \theta + 2 \cos^2 \theta - \cos^3 \theta}{2 - \cos \theta - \cos^3 \theta} \right\} \quad (51)$$

This is the required solution of the problem. It gives the change in deformation with force for a given contact angle and radii of the particle and of the undeformed bubble or droplet.

Discussion

It is hardly surprising that this result shows that the deformation of the bubble or droplet is linear in the force. After all, an expansion to linear order in F was invoked throughout. And in any case Hooke's law is a general statement about the thermodynamic stability of matter: the constrained thermodynamic potential is minimized by the equilibrium value of the constraint, and it is therefore a quadratic function near equilibrium,²¹ which means that *all* systems must behave as simple springs for sufficiently small perturbations. The two nontrivial questions are as follows: What is the value of the spring constant? What is the extent of the linear regime?

The spring constant of the bubble or droplet is defined as $k = -F/\Delta z(0)$. From eq 51 we obtain

$$k^{-1} = \frac{-1}{4\pi\gamma} \left\{ \ln \left[\frac{R_p}{2\kappa R_0^2} \frac{(1 + \cos \theta)^2}{\sin^2 \theta} \right] + \frac{4 - 5 \cos \theta + 2 \cos^2 \theta - \cos^3 \theta}{2 - \cos \theta - \cos^3 \theta} \right\} \quad (52)$$

The spring constant has a linear dependence on surface tension, and it also depends on the contact angle. The logarithmic dependence on size (particle radius, bubble or droplet radius, and interaction decay length) is very weak. (Evans et al.¹⁵ analyzed the effective spring constants of fluid membranes and found a similar logarithmic dependence on size for their particular pipet and capsule geometry.) As can be seen in Figure 2, the interfacial spring constant is a relatively slowly varying function of the interior contact angle. Using typical values (cf. refs 7 and 8), $R_0 = 0.25$ mm and $R_p = 6$ μ m and κ^{-1}

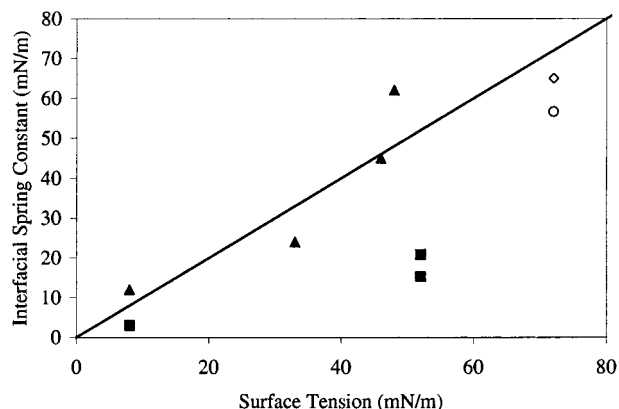


Figure 3. Spring constant of a bubble (empty symbols) or an oil droplet (filled symbols) as a function of the surface tension. The full line is $k = \gamma$. The symbols are measured AFM data given directly in ref 7 (triangles) and in ref 1 (diamond) and extracted from Figure 3 of ref 3 (circle) and from Figures 6 and 8 of ref 8 (squares).

= 10 nm, the ratio of length scales is $R_p k^{-1}/R_0^2 = 10^{-6}$, which gives a spring constant in the range $1-1.2\gamma$ for contact angles greater than 20° . (The spring constant diverges logarithmically for smaller contact angles.) Decreasing the size of the probe or the decay length of the interaction, or increasing the size of the bubble or drop, makes the interface softer; an order of magnitude decrease in the size ratio decreases the interfacial spring constant by about 15%.

The present analysis was carried out for small loads, $F/2\pi\gamma R_p \ll 1$. Typical force measurements show a linear regime and apply a maximum load corresponding to a value of this parameter in the range $1-4 \times 10^{-2}$, 7×10^{-3} to 10^{-2} ,⁸ and 7×10^{-3} .³ We conclude that the present analysis may be safely applied to the experimental data.

Figure 3 compares the predicted spring constant for a typical case with several AFM measurements of the interfacial spring constant. All of the experiments show interfacial spring constants that are of the same order as the surface tension. The data of Hartley et al.⁷ for oil droplets is particularly convincing. Not only is it clearly linear in the surface tension, but the constant of proportionality is close to unity. The present theory predicts a value of 0.95γ for the experimental size ratio of 5×10^{-7} and contact angle of 90° . The apparent differences between the constants of proportionality in the different systems most likely reflect the differences in the contact angles and differences in size ratio in each case. The reason for the rather low values of Aston and Berg⁸ are unclear. Over all the experimental data for both droplets and bubbles, the agreement is quite satisfactory and confirms that the most important contributions to the deformation have been included in the present analysis.

Summary and Conclusion

This paper has analyzed the deformation of a drop or bubble caused by a load applied by a particle or probe whose radius was much less than that of the fluid interface. Starting from the constrained thermodynamic potential, the load was expressed as an integral of the local pressure over the contact region, and the Euler–Lagrange equation

for the profile was derived. A feature of the analysis was that most of the results were obtained in terms of the applied load and were independent of the details of the force law. Exact results were obtained for the location of the dimple rim and for the maximum force that can be applied before rupture. An expression for the shape of the deformed profile in the region beyond the probe that was exact for weak forces was obtained. Perhaps the most surprising conclusion from the analysis was that the deformation of air bubbles was identical to that of liquid drops.

The profile in the region directly influenced by the interaction with the probe was also treated in the weak force regime for the case of an exponentially decaying force law, such as an electric double layer interaction. It was shown that the stiffening of the interface by the interaction was negligible. Expressions for the maximum local pressure and the minimum separation were obtained, as were expressions for the wrap radius and for the lateral extent of the interaction regime. These results were combined to give the height of the deformed interface in terms of the applied load.

The latter result yielded an explicit expression for the interfacial spring constant that was linear in the surface tension, that depended logarithmically on the radius of the probe, the radius of the droplet or bubble, and the decay length of the force law, and that depended weakly on the contact angle. For typical experimental values the interfacial spring constant is almost equal to the surface tension. It was also shown that the weak force regime analyzed here coincided with loads typically applied in experiments.

It is worth mentioning that the hookean response of the fluid interface is exact for weak forces, and it means that the height of the interface must vary linearly with the applied load. Since the minimum separation between the probe and the interface varies much more slowly than the drive distance as the load is increased (cf. eqs 45 and 47), atomic force microscopy experiments must show a regime where the force increases linearly with drive distance, as discussed following eq 1.²⁰ This also means that it is linear in the nominal separation, which is the drive distance less the deflection of the cantilever.¹⁶⁻¹⁹ In the very weak initial force regime, the variation in actual separation between the interface and the probe is of the same order as the change in drive distance, and the force is no longer a linear function of the drive distance or nominal separation. Nevertheless, the drop or bubble itself is still hookean, and when this variation in separation is taken into account using the equations given above, one can quantitatively describe the experimental data over the whole measurement regime.²⁶

We conclude from the present analysis and from the diverse experimental data shown in Figure 3 that bubbles or drops behave as hookean springs over experimental regimes and that the effective spring constant scales with the surface tension.

Acknowledgment. The support of the Australian Research Council is gratefully acknowledged.

LA010969G